European Journal of Wood and Wood Products (2021) 79:189–198
https://doi.org/10.1007/s00107-020-01616-8

ORIGINAL ARTICLE

Effects of aluminum sulfate soaking pretreatment on dimensional stability and thermostability of heat-treated wood

Lijie Qu[1] · Zhenyu Wang[1] · Jing Qian[1] · Zhengbin He[1] · Songlin Yi[1]

Received: 1 May 2020 / Accepted: 20 October 2020 / Published online: 4 November 2020

Abstract
Acidic aluminum sulfate hydrolysis solutions can be used to catalyze the thermal degradation of wood in a mild temperature environment, and thus reduce the temperature required for heat treatment process. To improve the dimensional and thermal stability of Chinese fir during heat treatment at 120 °C, 140 °C and 160 °C, this study investigated the effects of soaking pretreatment with 5%, 10% and 15% aluminum sulfate on the chemical and structural changes of the heat-treated Chinese fir. The results indicated that the samples treated at 15% aluminum sulfate concentration and 160 °C heat treatment achieved the best dimensional and thermal stability. Chemical analyses by Fourier transform infrared spectroscopy (FTIR) and X-ray diffraction (XRD) indicated that the catalysis of aluminum sulfate resulted in degradation of hemicelluloses during the heat treatment, and an increase in the soaking concentration and heat treatment temperature also affected the thermal degradation of celluloses. The scanning electron microscope (SEM) and mass changes test results proved that the hydrolyzed aluminum flocs mainly adhered to the inner wall of the wood tracheid as spherical precipitates, and when the soaking concentration reached 10% and 15%, a uniform soaking effect could be achieved. The thermogravimetric (TG) analysis revealed the soaking pretreatment effectively improved the thermal stability of the heat-treated wood by physically wrapping and promoting the formation of a carbon layer on the wood surface during heat treatment. Thus, aluminum sulfate soaking pretreatment exerted a great effect on the dimensional and thermal stability of wood, allowing heat treatment to be performed at a lower temperature.

Keywords Aluminum sulfate · Dimensional stability · Heat treatment · Soaking pretreatment · Thermal stability

1 Introduction

Approximately 70% of wood products are used as building materials, such as decorative frames for structures, doors, and windows, and floor and wainscot systems (Grosse et al. 2019; Jiang et al. 2018). The use of wood from sustainable plantations is an environmentally-friendly alternative to other construction materials such as concrete or steel, which generate large quantities of pollution during their production (Morreale et al. 2015). However, wood also presents several disadvantages, including deformation due to shrinkage and swelling, which reduce the stability of wood-based structures. Wood also is flammable, which makes it less safe compared to other materials (Chu et al. 2017).

Heat treatment is used to improve the dimensional stability, durability, and corrosion resistance of wood, as well as modify its color, which allows heat-treated wood to be used as an element in facades, terraces, urban furniture, and windows (Nguyen et al. 2018; Wang et al. 2015; Windeisen et al. 2007). Heat treatment accounts for 40–70% of the energy consumption of the entire wood production process and is typically conducted at 180–240 °C for 2–8 h (Aydemir et al. 2015; Huang et al. 2012a; Kol and Sefil 2011; Nuopponen 2005; Obataya et al. 2006). Environmental problems have become a major governmental and social concern, and burning waste products and biomass pellet fuels has been prohibited in cities with major wood processing factories (Watt et al. 2019). Thus, materials can only be heated using electricity, which is expensive and consequently increases the cost of wood processing. Temperature and duration are the two main factors that affect the heat treatment of wood. However, excessively high temperatures have

✉ Zhengbin He
hzbcailiao@bjfu.edu.cn

✉ Songlin Yi
ysonglin@bjfu.edu.cn

[1] Beijing Key Laboratory of Wood Science and Engineering, Beijing Forestry University, Beijing 100083, China

correspondingly higher requirements for equipment quality (Boonstra and Tjeerdsma 2006; Lee et al. 2018). Thus, reducing the temperature during heat treatment is a challenge in the wood industry.

The energy required for heat treatment can be reduced by pretreating heat-treated materials. Aluminum sulfate is widely used in the papermaking industry because of its good thermal stability, low toxicity, and low cost. Hydroxyl complexes are formed by hydrolysis in aluminum sulfate solutions and easily react with polar groups or become sweep-flocculated in the wood voids (Browne and Driscoll 1993; Irfan et al. 2013). Due to the presence of polar functional groups such as hydroxyls and carboxyls, wood can be impregnated by soaking it in an aluminum sulfate solution (Choudhary et al. 2015). Heat treatment is used to thermally degrade hemicellulose at high temperatures into acetic acid which further degrades cellulose, hemicellulose, and lignin by acid catalysis (Cermak et al. 2019; Yang et al. 2018). Acidic aluminum sulfate hydrolysis solutions can be used to catalyze the thermal degradation of wood in a low-temperature environment. Thermally stable hydrogenated hydroxides encapsulate and fill the wood, which increases its thermal stability and mechanical properties. Moreover, after being pretreated with aluminum sulfate, the thermal degradation rate of wood is accelerated, which reduces the heat treatment duration.

In this study, the authors aimed to obtain modified wood with good dimensional stability and thermostability by soaking pretreatment with chemical reagents using less complex and relatively mild reaction conditions (120−160 °C).

2 Materials and methods

2.1 Materials

Chinese fir (*Cunninghamia lanceolata* (Lamb.) Hook) obtained from a forest farm in Guangxi, China was selected as the raw material for the study. After air-drying, the wood was machined into the dimensions of 20 mm × 20 mm × 20 mm by Guangxi Ushine Home Products Ltd., Co. (Guangxi, China). The wood samples were prepared for 12 treatment groups. First, all samples were divided into four different soaking concentration groups (0%, 5%, 10% and 15%), and then each group was divided into three different temperature groups (120 °C, 140 °C and 160 °C). Twenty samples were prepared from each group. Prior to the tests, all of the samples were conditioned in a climate-controlled chamber (TH-270DH, Shandong, China) at 20 °C and 65% relative humidity to a moisture content of 12%, and this weight was recorded (W1). Aluminum sulfate solutions with mass fractions of 5%, 10%, and 15% were prepared by analytical grade aluminum sulfate [$Al_2(SO_4)_3$, 99.5%] and deionized water at 25 °C by stirring at 200 rpm/min for 15 min. Aluminum sulfate and deionized water were supplied by Sinopharm Chemical Reagent Co., Ltd. (Shanghai, China) and Beijing Lanyi chemical products Co., Ltd (Beijing, China), respectively.

2.2 Soaking pretreatment

All samples were divided into four groups and placed in a 2 L vessel and secured with a stainless steel mesh to keep the wood cubes immersed in solution: a control group (0% un-soaked), and the remaining three groups (soaked group) were immersed in 5%, 10%, or 15% aluminum sulfate solutions. Then aluminum sulfate soaking pretreatment was conducted in a vacuum drying oven (BPZ-6090Lc, Yiheng, Shanghai, China) at 25 °C, and the vacuum was maintained for 20 min at 0.04 MPa and then released. This soaking cycle was performed three times. The control group was subjected to the same treatment but was immersed in deionized water. Experiments were performed in triplicate, and the average was used for analysis.

2.3 Heat treatment

After soaking pretreatment, all soaking pretreated samples were dried in a drying oven (DHG-9023A, HUMGINE, Shanghai, CHINA) at 60 °C for 30 min and weighed (W2). After that, the 60 °C-dried samples with 0% (control group), 5%, 10%, and 15% aluminum sulfate soaking pretreatment were divided into three groups and individually heat-treated at three different temperature levels, 120 °C, 140 °C, and 160 °C, for 2 h controlled within ± 1 °C in a DHG Series Heating and Drying Oven (DHG-9205A, HUMGINE, Shanghai, CHINA) with saturated water vapor as the shield gas. After heat treatment, the weight (W3) and tangential and radial dimensions of the samples were measured. The wood samples with different treatments were analyzed and are listed in Table 1.

2.4 Mass changes

The weight percentage gain (WPG) of the samples was calculated using Eq. (1):

$$\mathrm{WPG}\ (\%) = \frac{W_2 - W_1}{W_1} \times 100 \tag{1}$$

where W_1 is the weight of wood samples before soaking treatment, and W_2 is the 60 °C dried weight of the soaked samples before heat treatment, respectively. Weight percentage loss (WPL) was also determined for all treated samples using Eq. (2):

Table 1 List of the samples studied under different treatment parameters

Sample (Chinese fir)	Al_2SO_3 concentration (%)	Heat treatment temperature (°C)/2 h
120 °C–0%	0 (un-soaked)	120
120 °C–5%	5	120
120 °C–10%	10	120
120 °C–15%	15	120
140 °C–0%	0 (un-soaked)	140
140 °C–5%	5	140
140 °C–10%	10	140
140 °C–15%	15	140
160 °C–0%	0 (un-soaked)	160
160 °C–5%	5	160
160 °C–-10%	10	160
160 °C–15%	15	160

$$\mathrm{WPL}\ (\%) = \frac{W_2 - W_3}{W_3} \times 100 \tag{2}$$

where W_2 is the 60 °C dried weight of the soaked samples before heat treatment, and W_3 is the weight of the soaked samples after heat treatment.

2.5 Dimensional stability measurements

The treated and control groups were oven-dried and stored in a climate-controlled chamber at 20 °C and 65% relative humidity to reach their equilibrium moisture content (EMC). The specimen dimensions were measured before and after conditioning (He et al. 2019). The swelling coefficient was calculated using Eq. (3):

$$a = \frac{l_w - l_0}{l_0} \times 100 \tag{3}$$

where a is the swelling coefficient (radial or tangential), l_0 denotes the initial dimension of the specimen, and l_w represents the dimension after conditioning.

Statistical data obtained from the dimensional stability tests were analyzed using SPSS 20.0 (SPSS Inc., Chicago, IL, USA). Differences between treatments were detected by ANOVA with the Student–Newman–Keuls (S-N-K) testing method. A p value < 0.05 was considered significant.

2.6 Characterization by Fourier transform infrared spectroscopy

Fourier-transform infrared spectroscopy was conducted (Tensor 27; Bruker, Bremen, Germany), and data were recorded in the 500–4000 cm^{-1} range with a resolution of 4 cm^{-1} for 32 scans. The background spectra of pure spectroscopy-grade KBr was subtracted from the sample spectra. The hydroxyl group peak (3340 cm^{-1}) was used to calculate the hydroxyl index (HI) using Eq. (4):

$$\mathrm{HI} = \frac{I_{3340}}{I_{1510}} \times 100 \tag{4}$$

where I_{3340} and I_{1510} denote the peak intensity at 3340 cm^{-1} and 1510 cm^{-1} respectively.

2.7 X-ray diffraction (XRD)

X-ray diffraction (XRD) was conducted using a D8 ADVANCE XRD (Bruker) with an accelerating voltage of 40 kV and a current of 40 mA. XRD patterns were obtained using Cu Kα radiation from $2\theta = 5°–60°$ at a scan rate of 4° min^{-1}. The crystallinity index (CI) and the apparent crystallite size (ACS) of Chinese fir samples were calculated using the Segal (Thygesen et al. 2005) and Scherrer methods (Newman 1999), respectively.

2.8 Analysis of thermal characteristics

Samples were milled through 60 mesh and used for thermogravimetric (TG) analysis. TG and derivative thermogravimetric (DTG) analyses were performed using a Netzsch STA449F3 computerized thermobalance (NETZSCH Gerätebau GmbH, Selb, Germany). Approximately 5 mg of samples were settled in an alumina crucible, and the temperature was increased to 900 °C at a rate of 10 °C/min.

2.9 Scanning electron microscopy (SEM)

The surface morphologies of the untreated, heat-treated, and soaking/heat-treated samples were analyzed by SEM (Hitachi S-3400N II, Tokyo, Japan). Chinese fir samples were coated with platinum by using a vacuum sputter coater before observation.

3 Results and discussion

3.1 Mass changes

3.1.1 Weight percentage gain

The WPG of the samples treated with different aluminum sulfate concentrations is shown in Fig. 1, which indicates that the WPG rate gradually increased with the soaking concentration. The significant increase in WPG for all samples soaked at different concentrations was attributed to the tendency of aluminum cations to react with polar

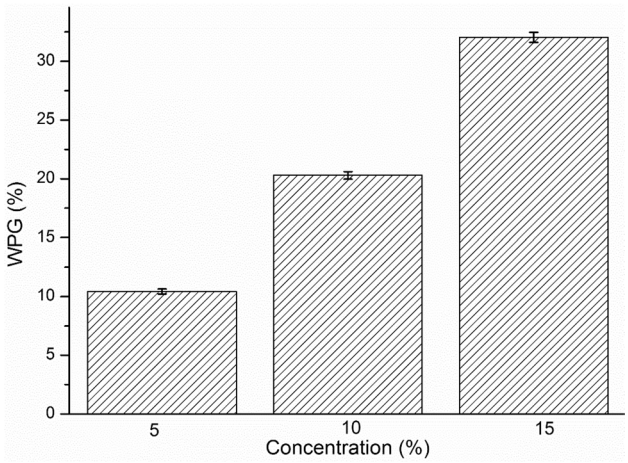

Fig. 1 Weight percentage gain (WPG) of samples

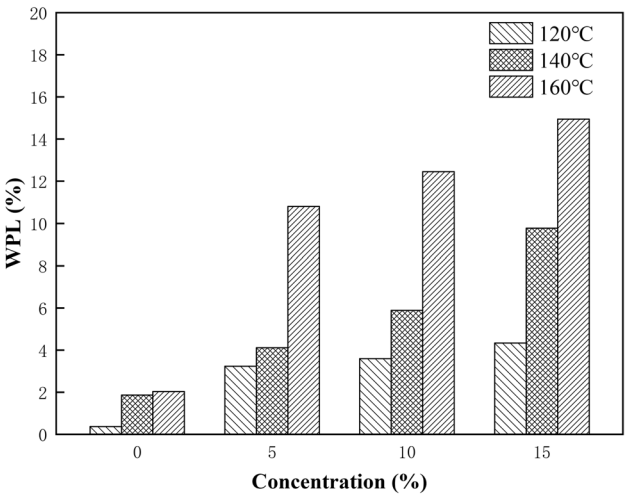

Fig. 2 Weight percentage loss of samples

groups—hydroxyl, phenolic, and carboxylic groups (Licskó 1993; Stumm and Morgan 1962). The effect—which may have resulted from sweep flocculation, adsorption, and bridging—can be enhanced as the pH is decreased in the presence of multivalent cations (Jekel 1986).

3.1.2 Weight percentage loss

Figure 2 shows that the control group (120 °C–0%, 140 °C–0%, 160 °C–0%) has a small WPL at 120 °C and increases significantly at 140 °C. Then, the WPL increased slightly at 160 °C. These results indicate that heat treatment at 120 °C only affected some of the volatile extracts in the un-soaked samples and exerted a milder effect on hemicellulose (Englund and Nussbaum 2000; Manninen et al. 2002). Hemicellulose degradation began at 140 °C, but the thermal degradation of hemicellulose did not change greatly between 140 and 160 °C.

After soaking, the WPL of the samples significantly increased compared with the control group. The WPL also increased as the soaking concentration increased at the same temperature. When heat-treated at 120 °C, the WPL in soaked samples significantly increased relative to the un-soaked samples, but changing the concentration only slightly affected the WPL. At the same soaking concentration, the WPL gradually increased upon increasing the temperature, but it was nearly the same under the following two sets of conditions: 120 °C–15% and 140 °C–5%; 140 °C–15% and 160 °C–5%. Thus, the aluminum sulfate soaking treatment exerted a catalytic effect on the heat treatment of wood, and the desired heat treatment effect was achieved at a reduced temperature.

3.2 Dimensional stability

Wood dimensional stability significantly influences the use and quality of wood products, and the swelling coefficients in the tangential and radial directions are the most significant factors for estimating the dimensional stability of wood (He et al. 2019). Figure 3 illustrates that aluminum sulfate soaking pretreatment and heat treatment influenced the dimensional stability of wood and shows that the swelling coefficients of the samples were markedly reduced after soaking pretreatment compared with the control group. After heat treatment at 140–160 °C, the swelling coefficients continuously decreased as the soaking concentration increased. These effects were attributed to the hydroxyls in the amorphous zone and hemicellulose, which are the key to the dimensional stability of samples. Aluminum sulfate catalyzes the thermal degradation of hemicellulose at low temperatures (Akgül et al. 2007); at higher temperatures, it also affects the amorphous regions of cellulose. Hydrolyzed aluminum flocs can be deposited in the amorphous regions and cell voids, such as the cell cavities, by complexation and sweep flocculation. Thus, it also exerts a physical bulking effect, which hinders contact between moisture and wood, and reduces the accessibility of hydroxyl groups, thereby improving the material's dimensional stability (Deka and Saikia 2000; Li et al. 2000).

The samples subjected to the 160 °C–15% treatment achieved the optimal dimensional stability. Moreover, compared with the 120 °C–0% sample, the swelling coefficients in the radial direction were reduced by 51.74% and 53.44%, respectively, and the swelling coefficients in the tangential direction were reduced by 49.62% and 48.86%, respectively. The dimensional stability of the 160 °C–15% sample was nearly identical to the 140 °C–15% sample, and the concentration showed a statistically significant effect on the swelling coefficients ($p < 0.05$), but the temperature did

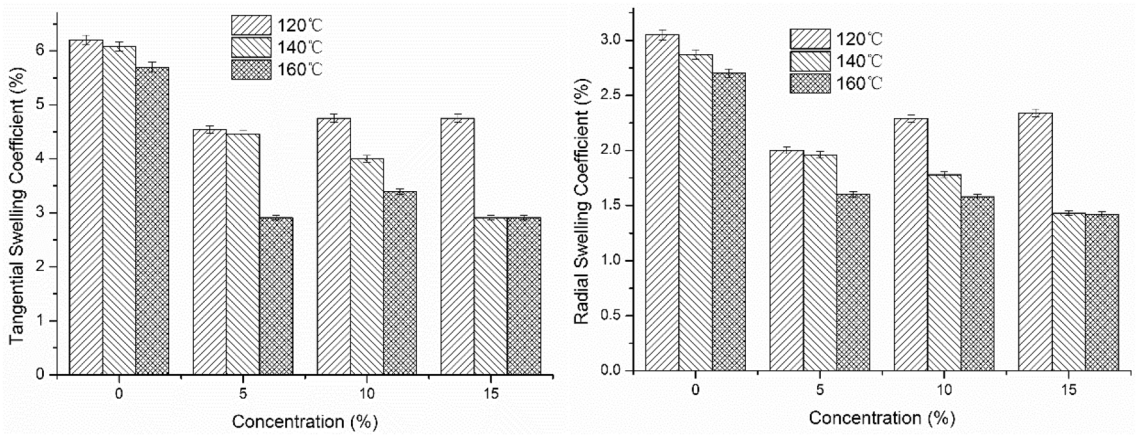

Fig. 3 Swelling coefficients in the tangential and radial directions for specimens treated under different conditions

not. This indicates that concentration had a greater effect on dimensional stability than temperature, and it also suggests that the soaking pretreatment can reduce the temperature of heat treatment.

3.3 Chemical structure analysis using Fourier transform infrared spectroscopy (FTIR)

The band at 1510 cm^{-1} was associated with aromatic skeletal vibrations, which is not much affected by heat treatment in the temperature range used in this study. Thus, all spectra were normalized to the band at 1510 cm^{-1} (Akgül et al. 2007; Srinivas and Pandey 2012). The band near 3340 cm^{-1} was assigned to hydrogen bonds, which strongly affect the dimensional stability of wood (Huang et al. 2013; Wei et al. 2018).

In Fig. 4, the hydroxyl index (HI) gradually decreased as the concentration increased in samples subjected to the same heat treatment temperature. This reduction indicates that the loss of hydroxyl group, and soaking pretreatment effectively catalyzed the degradation of hemicelluloses during treatment (Kondo 1997; Rautkari et al. 2013; Srinivas and Pandey 2012; Tjeerdsma et al. 1998; Weiland and Guyonnet 2003). The HI values obtained in the 120 °C–15% and 140 °C–15% treatments were significantly lower than those obtained in the 140 °C–0% and 160 °C–0% treatments. This was similar to the dimensional stability analysis and indicates that the soaking pretreatment allowed the samples to achieve a desired heat treatment effect at a lower temperature, thereby reducing the temperature required for heat treatment.

The peaks at 2918 cm^{-1} and 1369 cm^{-1} are the characteristic C–H stretching vibration peaks, and the peaks at 1733 cm^{-1} and 1595 cm^{-1} were assigned to C–O and aromatic carbon skeleton stretching vibrations, respectively (Huang et al. 2012b; Nguyen et al. 2019; Shou et al. 2014). The above peaks also changed after undergoing both soaking pretreatment and heat treatment, but the other functional groups did not change after the combined treatment. This shows that the combined treatment can change the chemical groups in the wood, while having little effect on the composition.

3.4 X-ray diffraction

X-ray diffraction patterns of control group and pretreated samples were obtained to investigate the crystallinity of the specimens. The crystallinity index (CI) and apparent crystallite size (ACS) of the samples are presented in Fig. 5. Three typical type I cellulose patterns with 101, 002, and 004 peaks were observed near $2\theta = 15°$, 22°, and 34°, respectively (Schorr et al. 2018; Wentzel et al. 2019).

In Fig. 5a, CI increased with temperature, and when the temperature reached 160 °C, the CI significantly increased. ACS showed a similar trend, but small changes were observed between 140 and 160 °C. The change between 120 and 140 °C was mainly attributed to the combination of crystalline regions in cellulose and because the crystal structure in wood became more ordered at 160 °C, thereby significantly increasing CI (Islam et al. 2011; Kim et al. 2010). In the soaking pretreatment group, as the heat treatment temperature increased, CI continuously increased at 5% soaking concentration (Fig. 5b), CI initially increased and then decreased when the soaking concentration reached 10% (Fig. 5c), and decreased continuously when the soaking concentration was increased to 15% (Fig. 5d). However, ACS decreased within each soaking concentration range. This could be due to the increase in soaking concentration and heat treatment temperature, which promoted the thermal degradation of hemicellulose and the pyrolysis of cellulose.

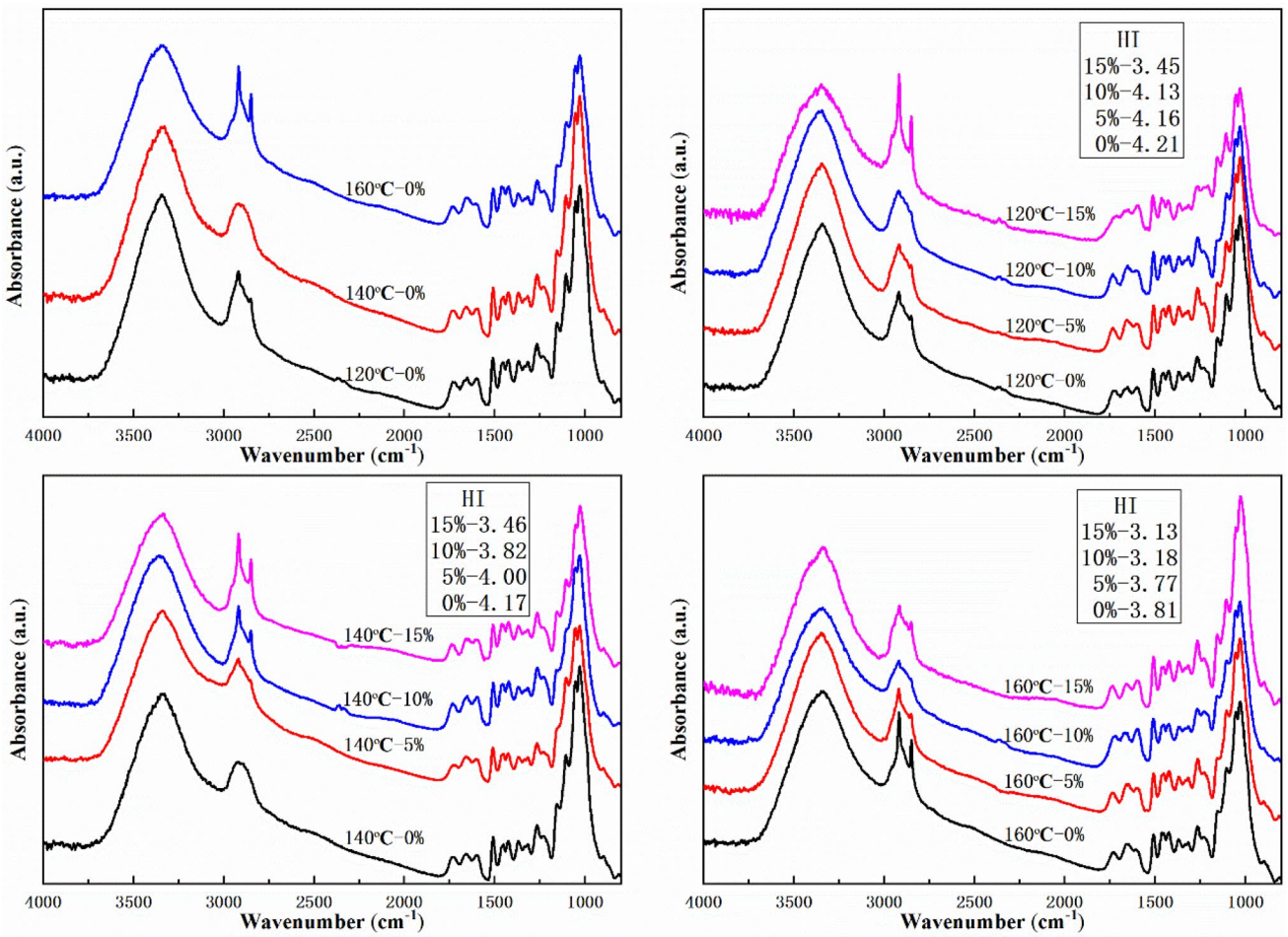

Fig. 4 FTIR spectra of samples in the control group and samples treated in different pretreatment soaking concentrations at the same heat treatment temperatures

3.5 Thermogravimetric analysis

Figure 6a shows the TG and DTG curves of the control group, and Fig. 6b–d) show the changes in the samples exposed to different soaking concentrations under the same heat treatment temperature. Figure 6a indicates that heat treatment of the samples from 120 to 160 °C only slightly affected their thermal stability. Simultaneously, a sub-reaction zone appeared at 600–700 °C in the soaking pretreated group but not in the control group. This reaction zone indicates that hydrolyzed aluminum flocs exhibited good heat resistance and slowly started thermal degradation at > 600 °C. It also shows changes in the residual weight loss rate (TG_{FPT}), temperature of the maximum thermal degradation rate (T_{M-DTG}), and maximum thermal degradation rate (*M-DTG*) of the sample in the main reaction zone in Table 2. The analysis indicates that TG_{FPT} increased with an increase in the soaking concentration, and T_{M-DTG} shifted to a lower temperature; however, the DTG curve of the soaked sample remained nearly unchanged under the same heat treatment conditions. The T_{M-DTG} of the soaked heat-treated sample shifted to a temperature (125.20 °C) that was lower than the control group. However, the initial thermal degradation temperature was nearly the same as the control group, and TG_{FPT} increased by about 75.31%, whereas the DTG decreased by about 65.71%. Samples treated below 160 °C–15% showed the greatest thermal stability; the TG_{FPT} increased by 105.59%, and the *M-DTG* decreased by 68.87% relative to the 120 °C–0% samples in the main reaction zone. Similar to the dimensional stability, the thermal stability of the 140 °C–15% sample was only slightly lower than the thermal stability of the 160 °C–15% samples. This difference may be attributed to the aluminum sulfate soaking pretreatment, which promoted the formation of a carbon layer on the wood surface during acid and heat treatment. This layer effectively hindered contact between the sample

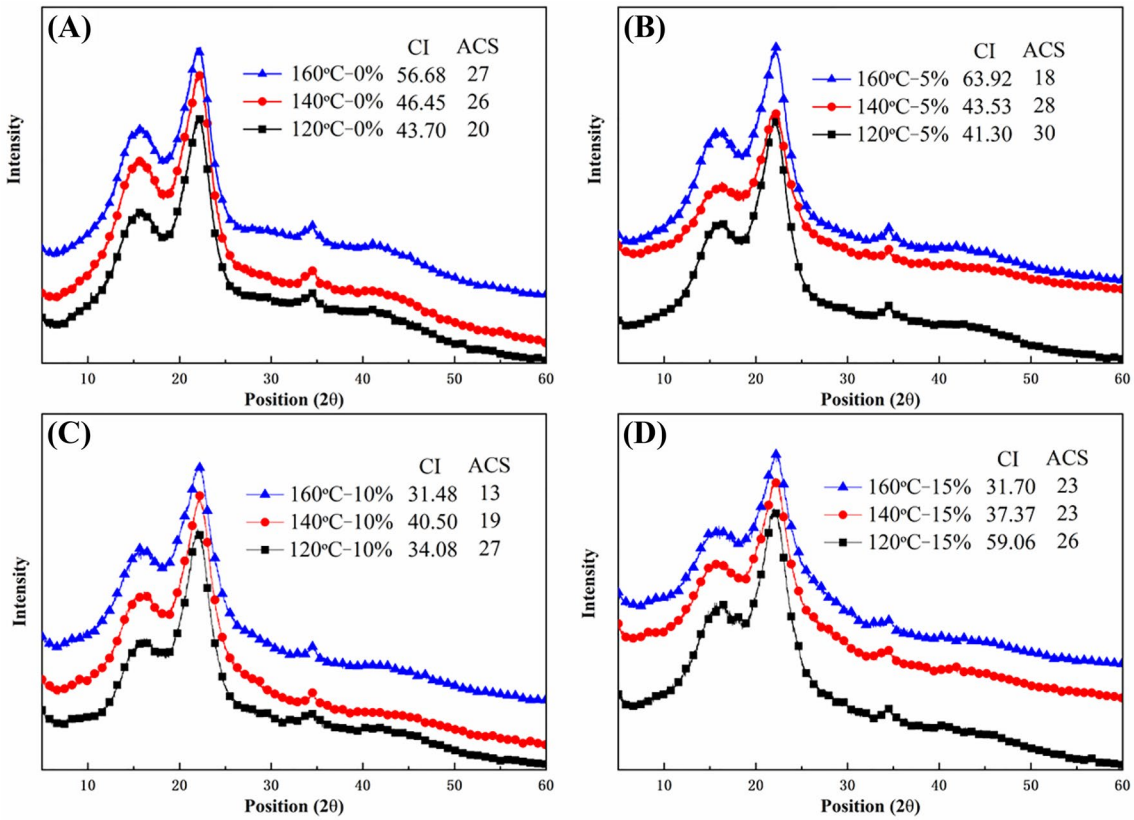

Fig. 5 Diffractograms of the samples after heat treatment at different temperatures with the same soaking concentration

and its environment (Lowden and Hull 2013; Wang et al. 2017, 2019). The hydrolyzed aluminum flocs protected the carbon layer and coated the flammable wood. The generation of acid during heat treatment and its retention in wood may have shifted T_{M-DTG} to a lower temperature, and the thermal degradation of the sample was catalyzed by a trace amount of acid during heating (Cai et al. 2018). Therefore, the soaking pretreatment effectively improved the thermal stability of the heat-treated wood.

3.6 Morphological characteristics

In aqueous solution, aluminum ions are first hydrolyzed to hydrated ions. During hydrolysis, H_2O ligands were gradually replaced by OH– to form hydroxide or hydroxide complex ions. Meanwhile, due to the formation of hydroxyl bridges, mononuclear complexes $pAl(OH)^{2+}$, $Al(OH)_2^{+}$ and $Al(OH)_4^{-}$] are gradually transformed into polynuclear hydroxide complexes [$Al_2(OH)_2^{4+}$, $Al_6(OH)_{15}^{3+}$, $Al_7(OH)_{17}^{4+}$, $Al_8(OH)_{20}^{4+}$, and $Al_{13}(OH)_{34}^{5+}$]. Finally, due to alternating hydrolysis and hydroxyl bridge reactions, a nearly insoluble aluminum hydroxide precipitate with a high degree of polymerization was generated:

$$[Al_n(OH)_{3n}] \rightarrow [Al(OH)_3]_n \downarrow$$

When the soaking concentration was 5%, the hydrolyzed aluminum flocs mainly adhered to the inner wall of the wood tracheid as spherical precipitates. When the soaking concentration reached 10% and 15%, the flocs were uniformly attached over a larger area, achieving a more complete soaking effect, which is also consistent with the WPG results. After heat treatment at 160 °C, the hydrolyzed aluminum flocs were still firmly attached to the inner wall of the tracheid, indicating that aluminum sulfate can fully participate in the reaction with wood during the heat treatment (Fig. 7).

4 Conclusion

The swelling coefficients of the samples decreased when the heat treatment temperature reached 140 °C and the soaking concentration was increased. The optimal dimensional stability was achieved by the 160 °C–15% sample. The SWR

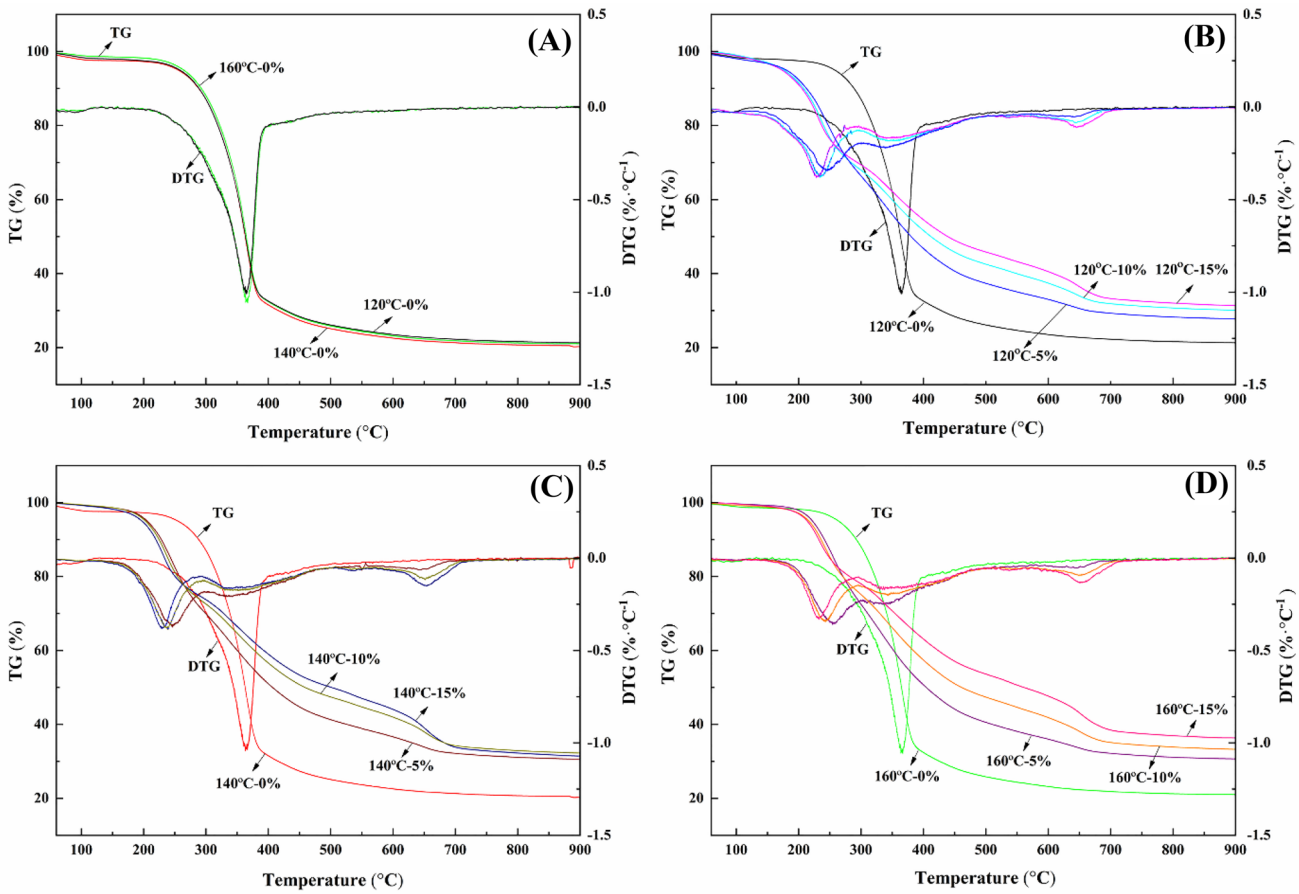

Fig. 6 Thermogravimetric (TG) and derivative thermogravimetric (DTG) curves of the samples

Table 2 Changes in the residual weight loss rate (TG_{FPT}, Temperature = 500 °C), temperature of the maximum thermal degradation rate (T_{M-DTG}), and maximum thermal degradation rate (*M-DTG*) of the samples in the main reaction zone

Sample	TG_{FPT} (%)	T_{M-DTG} (°C)	M-DTG (% °C^{-1})
120 °C–0%	26.81	366.98	1.06
120 °C–5%	38.74	246.32	0.33
120 °C–10%	43.91	234.70	0.38
120 °C–15%	47.18	230.28	0.38
140 °C–0%	26.05	363.36	1.04
140 °C–5%	42.73	246.31	0.37
140 °C–10%	48.84	237.13	0.38
140 °C–15%	51.50	228.70	0.38
160 °C–0%	26.81	363.79	1.05
160 °C–5%	42.07	255.92	0.35
160 °C–10%	48.93	243.50	0.34
160 °C–15%	55.12	232.69	0.33

and SHR of the samples in the radial direction were reduced by 51.74% and 53.44%, respectively, and those of the samples in the tangential direction were reduced by 49.62% and 48.86%, respectively, relative to the 120 °C 0% sample. The 140 °C–15% samples exhibited nearly the same dimensional stability as the 160 °C–15% sample.

Soaking pretreatment improved the thermal stability of Chinese fir samples, and the highest thermal stability was obtained in the 160 °C–15% samples. In the main reaction zone, the TG_{FPT} increased by 105.59%, and the M-DTG decreased by 68% relative to the 120 °C–0% samples. Moreover, both 140 °C–15% and 160 °C–15% samples showed similar improvements in the thermal stability, which is similar to the dimensional stability results. Thus, compared with heat treatment, soaking pretreatment exerted a greater effect on the dimensional and thermal stability of wood, allowing thermal treatment to

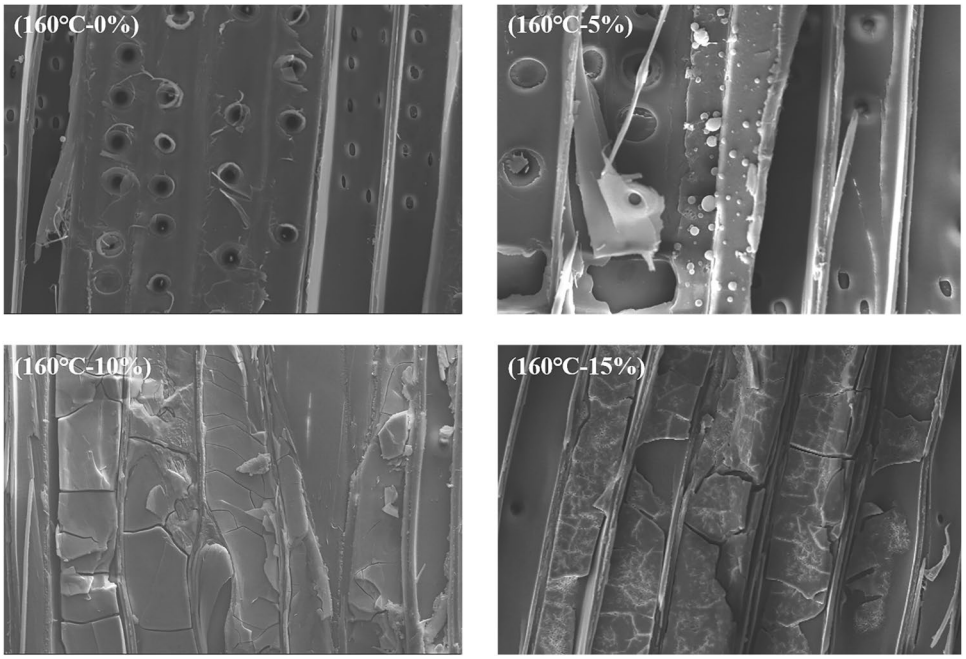

Fig. 7 Scanning electron micrograph of 160 °C heat-treated samples at different soaking concentrations

be performed at a lower temperature, thereby reducing the heat treatment temperature.

Author contributions LQ and ZH designed the experiments. LQ, ZW and JQ carried out the experiments. LQ and HZ analyzed the data and wrote this manuscript. SY gave valuable suggestions on the experiments and manuscript. LQ, ZW, ZH and JQ modified the manuscript in detail. All authors read and approved the final manuscript.

Funding This paper was supported by the China National Key R & D Program during the 13th Five-year Plan Period (2018YFD0600305); the Fundamental Research Funds for the Central Universities of China (2015ZCQ-CL-01); the Major Scientific and Technological Achievements Incubation Projects in Beijing Forestry University (2017CGP014) and the Hot Tracking Project in Beijing Forestry University (2017BLRD04).

Availability of data and material All data generated or analyzed during this study are included in this published article.

Compliance with ethical atandards

Conflict of interest The authors declare no conflicts of interest.

References

Akgül M, Gümüşkaya E, Korkut S (2007) Crystalline structure of heat-treated Scots pine [*Pinus sylvestris* L.] and Uludag fir [*Abies nordmanniana* (Stev.) subsp. *bornmuelleriana* (Mattf.)] wood. Wood Sci Technol 41:281–289

Aydemir D, Kiziltas A, Kiziltas EE, Gardner DJ, Gunduz G (2015) Heat treated wood-nylon 6 composites. Compos Part B Eng 68:414–423. https://doi.org/10.1016/j.compositesb.2014.08.040

Boonstra M, Tjeerdsma B (2006) Chemische analyse von wärmebehandeltem. Holz Roh Werkst 64:204–211

Browne BA, Driscoll CT (1993) pH-dependent binding of aluminum by a fulvic acid. Environ Sci Technol 27:915–922

Cai C, Antikainen J, Luostarinen K, Mononen K, Heräjärvi H (2018) Wetting-induced changes on the surface of thermally modified Scots pine and Norway spruce wood. Wood Sci Technol 52:1181–1193. doi:https://doi.org/10.1007/s00226-018-1030-1

Cermak P, Dejmal A, Paschova Z, Kymalainen M, Domeny J, Brabec M, Hess D, Rautkari L (2019) One-sided surface charring of beech wood. J Mater Sci 54:9497–9506. https://doi.org/10.1007/s10853-019-03589-3

Choudhary AK, Kumar S, Sharma C (2015) Removal of chloro-organics and color from pulp and paper mill wastewater by polyaluminium chloride as coagulant. Desalin Water Treat 53:697–708

Chu D, Mu J, Zhang L, Li Y (2017) Promotion effect of NP fire retardant pre-treatment on heat-treated poplar wood. Part 1: color generation, dimensional stability, and fire retardancy. Holzforschung 71(3):207–215. https://doi.org/10.1515/hf-2016-0082

Deka M, Saikia CN (2000) Chemical modification of wood with thermosetting resin: effect on dimensional stability and strength property. Biores Technol 73:179–181

Englund F, Nussbaum RM (2000) Monoterpenes in Scots pine and Norway spruce and their emission during kiln drying. Holzforschung 54:449–456

Grosse C, Grigsby WJ, Nol M, Treu A, Thevenon MF, Grardin P (2019) Optimizing chemical wood modification with oligomeric lactic acid by screening of processing conditions. J Wood Chem Technol 39:385–398. https://doi.org/10.1080/02773813.2019.1601739

He ZB, Qian J, Qu LJ, Yan N, Yi SL (2019) Effects of Tung oil treatment on wood hygroscopicity, dimensional stability and thermostability. Ind Crops Prod 140:6. https://doi.org/10.1016/j.indcrop.2019.111647

Huang X, Kocaefe D, Boluk Y, Kocaefe Y, Pichette A (2012a) Effect of surface preparation on the wettability of heat-treated jack pine wood surface by different liquids. Eur J Wood Prod 70:711–717

Huang XA, Kocaefe D, Kocaefe Y, Boluk Y, Pichette A (2012b) A spectrocolorimetric and chemical study on color modification of heat-treated wood during artificial weathering. Appl Surf Sci 258:5360–5369. doi:https://doi.org/10.1016/j.apsusc.2012.02.005

Huang X, Kocaefe D, Kocaefe Y, Boluk Y, Krause C (2013) Structural analysis of heat-treated birch (*Betule papyrifera*) surface during artificial weathering. Appl Surf Sci 264:117–127

Irfan M, Butt T, Imtiaz N, Abbas N, Khan RA, Shafique A (2013) The removal of COD, TSS and colour of black liquor by coagulation–flocculation process at optimized pH, settling and dosing rate. Arab J Chem 48:1103-1110.e1104

Islam MS, Hamdan S, Jusoh I, Rahman MR, Talib ZA (2011) Dimensional stability and dynamic Young's modulus of tropical light hardwood chemically treated with methyl methacrylate in combination with hexamethylene diisocyanate cross-linker. Ind Eng Chem Res 50(7):3900–3906. https://doi.org/10.1021/ie1021859

Jekel MR (1986) Interactions of humic acids and aluminum salts in the flocculation process. Water Res 20:1535–1542

Jiang JL, Bachtiar EV, Lu JX, Niemz P (2018) Comparison of moisture-dependent orthotropic Young's moduli of Chinese fir wood determined by ultrasonic wave method and static compression or tension tests. Eur J Wood Prod 76:953–964. https://doi.org/10.1007/s00107-017-1269-5

Kim UJ, Eom SH, Wada M (2010) Thermal decomposition of native cellulose: influence on crystallite size. Polym Degrad Stab 95:778–781

Kol HS, Sefil Y (2011) The thermal conductivity of Fir and beech wood heat treated at 170, 180, 190, 200, and 212 °C. J Appl Polym Sci 121:2473–2480. https://doi.org/10.1002/app.33885

Kondo T (1997) The assignment of IR absorption bands due to free hydroxyl groups in cellulose. Cellulose 4:281–292. https://doi.org/10.1023/A:1018448109214

Lee SH, Ashaari Z, Lum WC et al (2018) Thermal treatment of wood using vegetable oils. A review. Constr Build Mater 181:408–419

Li JZ, Furuno T, Katoh S (2000) Dimensional stability and flame resistance of silicate-acetylated and -propionylated wood composites. J Wood Chem Technol 20:441–453

Licskó I (1993) Dissolved organics removal by solid-liquid phase separation (adsorption and coagulation). Waterence Technol 27:245–248

Lowden LA, Hull TR (2013) Flammability behaviour of wood and a review of the methods for its reduction. Fire Sci Rev 2:4

Manninen AM, Pasanen P, Holopainen JK (2002) Comparing the VOC emissions between air-dried and heat-treated Scots pine wood. Atmos Environ 36:1763–1768

Morreale M, Liga A, Mistretta MC, Ascione L, Mantia FP (2015) Mechanical, thermomechanical and reprocessing behavior of green composites from biodegradable polymer and wood flour. Materials 8:7536

Newman RH (1999) Estimation of the lateral dimensions of cellulose crystallites using 13C NMR signal strengths solid state. Nuclear Magn Reson 15:21–29

Nguyen THV, Nguyen TT, Ji XD, Nguyen VD, Guo MH (2018) Enhanced bonding strength of heat-treated wood using a cold atmospheric-pressure nitrogen plasma jet. Eur J Wood Prod 76:1697–1705. doi:https://doi.org/10.1007/s00107-018-1351-7

Nguyen TT, Nguyen THV, Ji XD, Yuan BN, Trinh HM, Do KTL, Guo MH (2019) Prediction of the color change of heat-treated wood during artificial weathering by artificial neural network. Eur J Wood Prod 77:1107–1116. doi:https://doi.org/10.1007/s00107-019-01449-0

Nuopponen M (2005) FT-IR and UV Raman Spectroscopic Studies on Thermal Modification of Scotch Pine Wood and Its Extractable. Compounds 951-22-7605–4

Obataya E, Shibutani S, Hanata K, Doi S (2006) Effects of high temperature kiln drying on the practical performances of Japanese cedar wood (*Cryptomeria japonica*) II: changes in mechanical properties due to heating. J Wood Sci 52:111–114

Rautkari L, Hill CAS, Curling S, Jalaludin Z, Ormondroyd G (2013) What is the role of the accessibility of wood hydroxyl groups in controlling moisture content? J Mater Sci 48:6352–6356

Schorr D, Blanchet P, Essoua GGE (2018) Glycerol and citric acid treatment of lodgepole pine. J Wood Chem Technol 38:123–136. https://doi.org/10.1080/02773813.2017.1388822

Shou GZ, Zhang WY, Gu YQ, Zhao DX (2014) Application of near infrared spectroscopy for discrimination of similar rare woods in the Chinese market. J Near Infrared Spectrosc 22:423–432

Srinivas K, Pandey KK (2012) Photodegradation of thermally modified wood. J Photochem Photobiol B-Biol 117:140–145. doi:https://doi.org/10.1016/j.jphotobiol.2012.09.013

Stumm W, Morgan JJ (1962) Chemical aspects of coagulation. J Am Water Work Assoc 54:971–994

Thygesen A, Oddershede J, Lilholt H, Thomsen AB, Ståhl K (2005) On the determination of crystallinity and cellulose content in plant fibres. Cellulose 12:563

Tjeerdsma B, Boonstra M, Pizzi AP, Tekely P, Militz H (1998) Characterisation of thermally modified wood: molecular reasons for wood performance improvement. Holz Roh Werkst 56:149-153.56. https://doi.org/10.1007/s001070050287

Wang W, Zhu Y, Cao JZ, Sun WJ (2015) Correlation between dynamic wetting behavior and chemical components of thermally modified wood. Appl Surf Sci 324:332–338. doi:https://doi.org/10.1016/j.apsusc.2014.10.139

Wang N, Liu Y, Xu C, Liu Y, Wang Q (2017) Acid-base synergistic flame retardant wood pulp paper with high thermal stability. Carbohydr Polym 2017:S014486171730975X. https://doi.org/10.1016/j.carbpol.2017.08.099

Wang YC, Zhao JP, Meng XJ (2019) Effect of expandable graphite on polyester resin-based intumescent flame retardant coating. Prog Org Coat 132:178–183. doi:https://doi.org/10.1016/j.porgcoat.2019.03.050

Watt MS, Kirschbaum MUF, Moore JR, Grant PH, Bulman LS, Brockerhoff EG, Nathanael M (2019) Assessment of multiple climate change effects on plantation forests in New Zealand. Forestry

Wei XY, Tao DH, Sheng XL, Zhang MH (2018) Modification of poplar wood using polyhexahydrotriazine and its effect on hygroscopicity. J Wood Chem Technol 38:214–223. https://doi.org/10.1080/02773813.2018.1432654

Weiland JJ, Guyonnet R (2003) Study of chemical modifications and fungi degradation of thermally modified wood using DRIFT spectroscopy. Holz Roh- Werkst 61:216–220

Wentzel M, Rolleri A, Pesenti H, Militz H (2019) Chemical analysis and cellulose crystallinity of thermally modified Eucalyptus nitens wood from open and closed reactor systems using FTIR and X-ray crystallography. Eur J Wood Prod 77:517–525. doi:https://doi.org/10.1007/s00107-019-01411-0

Windeisen E, Strobel C, Wegener G (2007) Chemical changes during the production of thermo-treated beech wood. Wood Sci Technol 41:523–536. doi:https://doi.org/10.1007/s00226-007-0146-5

Yang Y, Dong CL, Luo B, Chen TA, Lu JX (2018) Characterization of wood surface elemental compositions after thermo-vacuum treatment and superheated-steam heat treatment. Bioresources 13:1895–1908. https://doi.org/10.15376/biores.13.1.1895-1908